

FUNCTIONALIZED RARE EARTH DOPED NaMnF₃ NANORODS; FACILE SYNTHESIS AND MULTICOLOR FINE TUNING OF POTENTIAL BIMODAL BIOPROBES

A. ABDULLAH^{a,b,*}, M. ANIS-UR-REHMAN^b, A. S. SALEEMI^{c,d}

^a*School of Science, University of Management and Technology, Sialkot Campus, Sialkot 51310, Pakistan*

^b*Applied Thermal Physics Laboratory, Department of Physics, COMSATS University, Islamabad 44000, Pakistan*

^c*Institute for Advanced Study, Shenzhen University, Shenzhen, Guangdong, China 518060. Key Laboratory of Advanced Materials (MOE)*

^d*School of Materials Science and Engineering, Tsinghua University, Beijing 100084, People's Republic of China*

The synthesis and upconversion fluorescence of NaMnF₃: Yb, Er/Tm is being reported here. A one step solvothermal method was utilized to prepare surface modified nanorods. The x-ray diffraction revealed the structure of prepared samples to be orthorhombic and transmission electron microscopy confirmed the nanorod morphology. The intense green, red and near-infra-red emissions were observed with change of dopant and dopant concentration.

(Received March 11, 2019; Accepted August 12, 2019)

Keywords: Crystal growth, Nanocrystalline materials, Functional, Biomaterials, Spectroscopy, Luminescence

1. Introduction

The scientists and researchers have interest in lanthanide doped upconversion (UC) nanocrystals (NCs). The attraction in these NCs is due to their superiority on conventional imaging probes because of their fascinating chemical and optical properties [1-2]. These become more desirable due to their multifunctionality as bimodal probes [3]. Optical imaging is one of the many modalities being used like positron emission tomography (PET), computed tomography (CT), magnetic resonance imaging (MRI) and ultrasound (US) [4]. Optical imaging is non-damaging, high sensitive and low cost technique. The advantages include minimum autofluorescence background, large anti-Stokes shifts, narrow emission bandwidths, light resistance to photo bleaching, non-blinking, excitation and emission in near-infra-red (NIR) region referred to as biological window or optical transmission window (700-1000 nm) [5].

Inorganic fluorides and oxides are being studied as host materials for lanthanides having chemical stability because of their low phonon energies specially AREF₄ (A = alkaline, RE = rare earth) [6]. Lanthanide doped materials are non-toxic unlike other imaging quantum dots [1]. The dispersivity and attachment with biological specimens is achieved through surface modifications with some suitable polymers. Various synthesis methods, specially wet chemical techniques are utilized to get nanocrystals with better dispersivity and narrow size distribution. The synthesis is normally a tiresome practice with multi steps involved [7-12].

Herein, the nanorods of NaMnF₃: Yb; Er/Tm were synthesized through a single step facile technique with surface modification. These were achieved with solvothermal method in which ethylene glycol was used as stabilizing agent. The surface modification was done in the same step of synthesis using polyethyleneimine (PEI). The ratios of dopants were fine tuned to obtain red and NIR emissions along with green and blue by exploiting the ladder like energy levels of

* Corresponding author: ali.abdullah@skt.umt.edu.pk

Yb:Er/Tm. The presence of Mn^{3+} made these structures effective potential candidates for bimodal imaging. This material has advantage over $AREF_4$ as fluorescence levels of Yb:Er/Tm are exploited for imaging and magnetic response of Mn is utilized for MRI. The magnetic response of $NaMnF_3$: Yb; Er/Tm is found even better than the $NaGdF_4$ which is considered as one of the best materials for dual modality as reported by Zhang et al [12].

2. Experimental

2.1. Synthesis

The solvothermal approach [13-14] was utilized to synthesize elongated structures of $NaMnF_3$. NH_4F , $NaCl$ and $MnCl_2$ (Aldrich made, analytical grade) were used to get F, Na and Mn ions respectively. Ethylene Glycol was used to stabilize the ions and PEI was used as polymer to render nanorods hydrophilic. Yb and Er were doped from lanthanides to achieve fluorescence and transition metal Mn was used for magnetic response. The Manganese is chosen as good biocompatibility is anticipated due to its presence in living organisms.

2.2. Reaction

Ethylene Glycol + $NaCl$ (sonication)

+

$MnCl_2$ + $Yb(NO_3)_3$ + $ErCl_3$ +PEI + NH_4F + Ethylene Glycol (sonication)



Hydrothermal treatment @200 °C for 2hr



Collection of particles, washing, drying @50 °C

2.3. Growth

The elongated structures have more intense emissions than the other NC structures [15]. Although the lack of in situ studies of solvothermal process [16], made it difficult to describe the growth mechanism but the elongated structured growth can be attributed to crystal structures of the reactants, ethylene glycol as solvent [17], heat treatment temperature, heat treatment time and pressure [18,19]. The fluoride source also favored the elongated growth [20, 6]. Moreover, the shape evolution of crystals is dependent on the compromise of the free energies of the faces of the crystals as explained by the Curie-Wulff-Gibbs model [21].

3. Results and discussion

The x-ray diffraction (XRD) was done on as-prepared samples of $NaMnF_3$:Yb/Er. The obtained pattern were indexed with reference pattern PDF-number 00-018-1224, having orthorhombic crystal system and space group number 62. The represented pattern is shown in figure 1. Transmission electron microscopy (TEM) revealed the nanorod structures with diameter range 50-80 nm. The represented images are given in figure 2. The XRD patterns were collected on Advance Bruker powder x-ray diffractometer with $Cu K\alpha$ radiation. The TEM images were taken using JEOL JEM-2100F. It is a difficult task to obtain NCs capable of single UC emission with high purity because lanthanide ions generally have more than one metastable excited state [22].

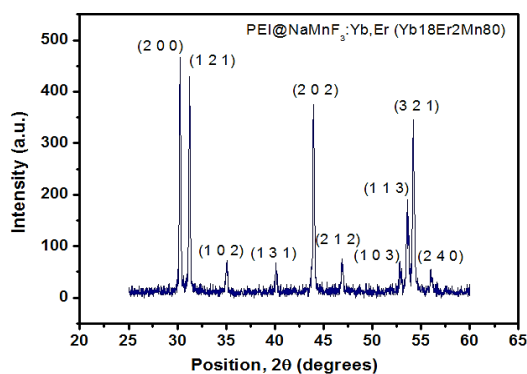


Fig. 1. XRD pattern of PEI-capped $\text{NaMnF}_3:\text{Yb,Er}$.

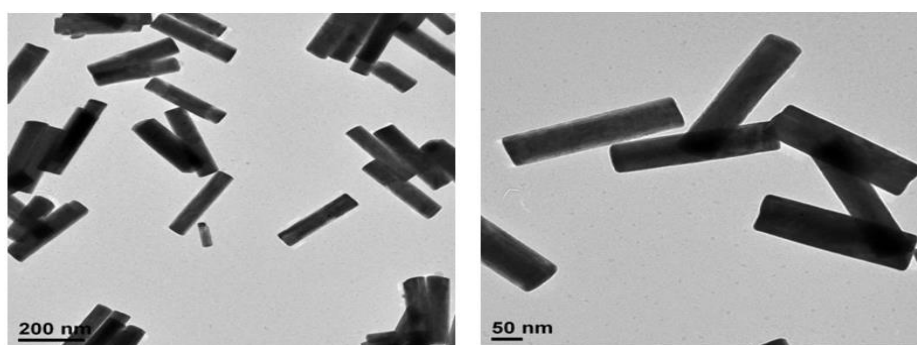


Fig. 2. TEM images for PEI- $\text{NaMnF}_3:\text{Yb,Er}$; Yb:Er 60/2 Mn 38 mol %.

For Yb/Er co-doped systems, a bright green emission (ca. 550 nm) was obtained with a weak dark red emission (ca. 660 nm) [23]. This becomes a limit for tissue imaging applications because of the low penetration depth of green and low intensity of red emission. The pure red emission is preferred as a probe for in vivo imaging since it can penetrate deep into tissues [22].

Fig. 3 shows the fluorescence spectra for $\text{NaMnF}_3:\text{Yb,Er}$. The red (${}^4\text{F}_{9/2} \rightarrow {}^4\text{I}_{15/2}$) emission is observed for Yb/Er 20/2. The increase in Yb concentration gave rise to dual band red and green (${}^4\text{S}_{3/2} \rightarrow {}^4\text{I}_{15/2}$) emissions with green band dominating. To further tune the red emission obtained at Yb 20, the concentration of Er was varied. The 10 and 20 mol % increase in Er gave rise to high intensity red emissions as shown in Fig. 4. Both the green and red emissions in respective samples were seen with naked eyes when excited by 980 nm laser. With such intense emissions it can be anticipated that the deep tissue penetration is achievable.

As the concentration of Yb increased, the intensity of the green emission became dominant. The green emission shown is of Yb80 Mn18 Er2.

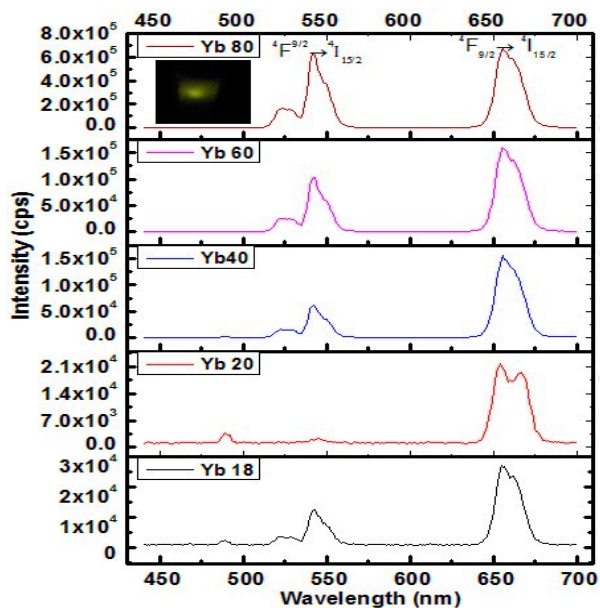


Fig. 3. Upconversion spectra of $\text{NaMnY}_3:\text{Yb,Er}$ capped with PEI for different molar percentage. Dominating enough red emission is obtained for Yb20 Mn78 Er2.

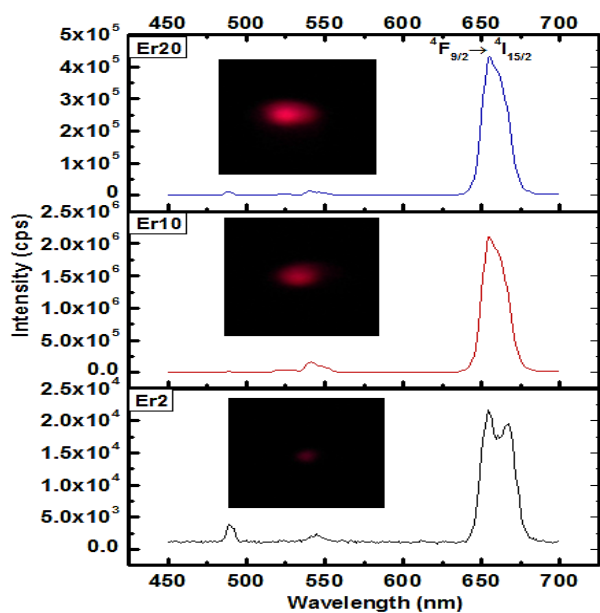


Fig. 4. Upconversion spectra of $\text{NaMnY}_3:\text{Yb,Er}$ capped with PEI for different molar percentage. Dominating red emission is obtained for increase in Er concentration with fixed concentration of Yb20.

The fluorescence properties were studied on Fluoromax-4 Horiba Jobin von Spectrofluorometer. The red UC emission obtained suggest that the exchange-energy transfer process between the Er^{3+} and Mn^{2+} ions is extremely efficient, which could be attributed to the resonances between the Mn^{2+} absorption bands and several metastable Er^{3+} levels in the crystal host lattices. The fine-tuning of red emission could be attributed to nonradiative energy transfer from the $^2\text{H}_{9/2}$ and $^4\text{S}_{3/2}$ levels of Er^{3+} to the $^4\text{T}_1$ level of Mn^{2+} , followed by back-energy transfer to the $^4\text{F}_{9/2}$ level of Er^{3+} , which improved the probability of the red emission transition [13,24-25]. The fluorescence increase and decrease was found non-linear. Also, with increase of Mn, the

fluorescence intensity decreased due to quenching phenomenon which happened due to efficient energy transfer among dopant ions [12].

For $\text{NaMnF}_3:\text{Yb,Tm}$ blue emission was observed for fixed Tm 0.02 and changing Yb, Mn concentration as shown in Fig. 5. The observed strong emission is NIR ${}^3\text{H}_4$ to ${}^3\text{H}_6$ [25-26] which might be due to energy transfer from ${}^1\text{D}_2$ and ${}^1\text{G}_4$ followed by back-energy transfer to the ${}^3\text{F}_4$ level [27].

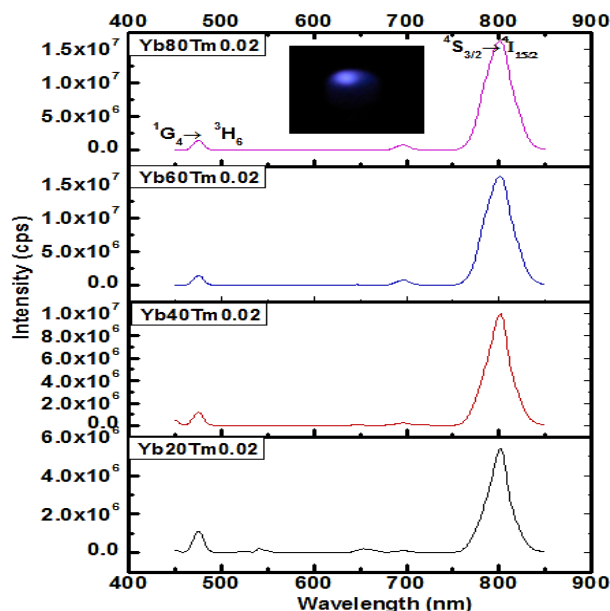


Fig. 5. Upconversion of Tm doped PEI capped $\text{NaMnF}_3:\text{Yb,Tm}$. The blue emission shown is of Yb80Tm0.02.

4. Conclusions

The synthesis and surface modification of NaMnF_3 co-doped with Yb;Er/Tm was successfully achieved in single step through solvothermal method. The PEI polymer was used for surface modification. An intense green emission was observed for $\text{NaMnF}_3:\text{Yb, Er}$, with increase in Yb concentration and for fixed Er at 2 mol%. The observed emission was around 550 nm between levels ${}^4\text{S}_{3/2}$ and ${}^4\text{I}_{15/2}$. Yb20 Mn78 Er2 revealed red emission at 660 nm between levels ${}^4\text{F}_{9/2}$ and ${}^4\text{I}_{15/2}$ which became intense with increase of Er concentration. With Tm as dopant, near IR emission was observed at 800 nm between levels ${}^3\text{H}_4$ and ${}^3\text{H}_6$ along with blue emission at 480 nm between energy levels ${}^1\text{G}_4$ and ${}^3\text{H}_6$. The XRD confirmed the structure to be orthorhombic and TEM showed the morphology to be nanorods.

Acknowledgements

This work is part of PhD research work done under Indigenous PhD program of Higher Education Commission (HEC), Pakistan. HEC is acknowledged for the financial support provided to A. Abdullah to visit Nanyang Technological University, Singapore, through International Research Support Initiative Program (HEC IRSIP). Prof. T. Y. T. Timothy and Dr. Y. Zhang of the School of Chemical and Biomedical Engineering, Nanyang Technological University, Singapore are thankfully acknowledged for facilitation provided there.

References

- [1] J. Shen, L. Zhao, G. Han, *Advance Drug Delivery Review* **65**, 744 (2013).
- [2] M. A. Hahn, A. K. Singh, P. Sharma, S. C. Brown, B. M. Moudgil, *Anal. Bioanal. Chem.* **399**, 3 (2011).
- [3] W. T. Ren, L. B. Liang, F. Qi, Z. B. Sun, Z. Y. Yang, X. Q. Huang, Q. Z. Wu, H. Y. Zhu, X. F. Yu, H. Quan, Q. Y. Gong, *J. Nanomater* **2011**, 531217 (2011).
- [4] D.-E. Lee, H. Koo, I.-C. Sun, J. H. Ryu, K. Kim, I. C. Kwon, *Chem. Soc. Rev.* **41**, 2656 (2012).
- [5] H. S. Mader, P. Kele, S. M. Saleh, O. S. Wolfbeis, *Current. Opinion. in Chem. Bio.* **14**, 582 (2010).
- [6] J. Liu, X. Liu, X. Kong, H. Zhang, *J. Solid. State. Chem.* **190**, 98 (2012).
- [7] H.-S. Qian, Y. Zhang, *Langmuir* **24**, 12123 (2008).
- [8] Z. Wang, C. Liu, L. Chang, Z. Li, *J. Mater. Chem.* **22**, 12186 (2012).
- [9] C. Li, J. Lin, *J. Mater. Chem.* **20**, 6831 (2010).
- [10] J. Zhou, Y. Sun, X. Du, L. Xiong, H. Hu, F. Li, *Biomaterials* **31**, 3287 (2010).
- [11] T. Cao, Y. Yang, Y. Gao, J. Zhou, Z. Li, F. Li, *Biomaterials* **32**, 2959 (2011).
- [12] Y. Zhang, J. D. Lin, V. Vijayaragavan, K. K. Bhakoo, T. Y. T. Tan, *Chem. Commun.* **48**, 10322 (2012).
- [13] F. Wang, X. Liu, *Chem. Soc. Rev.* **38**, 976 (2009).
- [14] J. Jin, Y.-J. Gu, C. W.-Y. Man, J. Cheng, Z. Xu, Y. Zhang, H. Wang, V. H.-Y. Lee, S. H. Cheng, W.-T. Wong, *ACS Nano* **5**, 7838 (2011).
- [15] J.-H. Zeng, J. Su, Z.-H. Li, R.-X. Yan, Y.-D. Li, *Adv. Mater.* **17**, 2119 (2005).
- [16] C. Tyrsted, K. M. Ø. Jensen, E. D. Bøjesen, N. Lock, M. Christensen, S. J. L. Billinge, B. B. Iversen, *Angew, Chem. Int. Ed.* **51**, 9030 (2012).
- [17] X. Jiang, Y. Wang, T. Herricks, Y. Xia, *J. Mater. Chem.* **14**, 695 (2004).
- [18] X. Wang, Y. Li, *J. Am. Chem. Soc.* **124**, 2880 (2002).
- [19] X. Wang, Y. Li, *Chem. Eur. J.* **9**, 5627 (2003).
- [20] C. Li, J. Yang, Z. Quan, P. Yang, D. Kong, J. Lin, *Chem. Mater.* **19**, 4933 (2007).
- [21] J. W. Mullin, *Crystallization*, Butterworth Heinmann, Oxford, 2001.
- [22] G. Tian, Z. Gu, L. Zhou, W. Yin, X. Liu, L. Yan, S. Jin, W. Ren, G. Xing, S. Li, Y. Zhao, *Adv. Mater* **24**, 1226 (2012).
- [23] A. Bednarkiewicz, D. Wawrzynczyk, M. Nyk, M. Samoć, *J. Rare. Earth* **29**, 1152 (2011).
- [24] J. Chen, J. X. Zhao, *Sensors* **12**, 2414 (2012).
- [25] S. Liang, Y. Liu, Y. Tang, Y. Xie, H. Sun, H. Zhang, B. Yang, *J. Nanomater* **2011**, 302364 (2011).
- [26] M. Nyk, R. Kumar, T. Y. Ohulchanskyy, E. J. Bergey, P. N. Prasad, *Nano. Lett.* **8**, 3834 (2008).
- [27] A. Yin, Y. Zhang, L. Sun, C. Yan, *Nanoscale* **2**, 953 (2010).